

WP2 - 2:30

SELECTION OF NEAR-MINIMUM TIME GEOMETRIC PATHS FOR ROBOTIC MANIPULATORS

Kang G. Shin and Neil D. McKay

Department of Electrical and Computer Engineering
The University of Michigan
Ann Arbor, Michigan 48109

ABSTRACT

A number of *trajectory* or *path planning* algorithms exist for calculating the joint positions, velocities, and torques which will drive a robotic manipulator along a given *geometric path* in minimum time. However, the time depends upon the geometric path, so the traversal time of the path should be considered again for geometric planning. There are algorithms available for finding minimum distance paths, but even when obstacle avoidance is not an issue minimum (Cartesian) distance is not necessarily equivalent to minimum time.

In this paper, we have derived a lower bound on the time required to move a manipulator from one point to another, and determined the form of the path which minimizes this lower bound. As a numerical example, we have applied the path solution to the first three joints of the Bendix PACS arm, a cylindrical robot. This example does indeed demonstrate that the derived approximate solutions require less time than Cartesian straight-line (minimum-distance) paths and joint-interpolated paths, i.e. those paths for which joint positions q^i are given by $q^i = a^i + b^i \lambda$.

1. INTRODUCTION

Productivity increase is the goal of the utmost importance in contemporary automation with programmable robotic manipulators. Driving robotic manipulators as fast as possible, i.e. minimum time control of manipulators, is an important means of achieving this goal. Minimum time control of manipulators generates several interesting but difficult control and planning problems. This paper is intended to treat one such problem, that is, minimum time geometric path planning for manipulators.

Loosely speaking, the problem of minimum time control (MTC) of a manipulator is concerned with the determination of control signals that will drive the manipulator from a given initial configuration to a given final configuration in as

The work reported here is supported in part by the NSF grant No. ECS-8409938 and the US AFOSR contract No. F49620-82-C-0089. Any opinions, findings, and conclusions or recommendations in this paper are those of the authors and do not necessarily reflect the view of the funding agencies.

short a time as possible, given constraints on the magnitudes of the control signals and constraints on the intermediate configurations of the manipulator, i.e., given that the manipulator must not hit any obstacles. In general, it is extremely difficult, if not impossible, to obtain an exact closed form solutions to the MTC problem due mainly to (i) the nonlinearity and coupling in the manipulator dynamics and (ii) the complexity involved with collision avoidance. One way to sidestep the collision avoidance problem (ii) is to assume that the desired geometric or spatial path has been specified *a priori*. As to the difficulty (i), although there are a few suboptimal solutions derived using approximate manipulator dynamics [2,3], the MTC problem is usually divided into two subproblems, i.e., *trajectory (or path) planning* and *trajectory (or path) tracking*, each of which is then solved separately. From a *task planner* we obtain a collision-free path in Cartesian space. This path is *transformed* to the corresponding path in joint space, giving a *geometric path* which is a parameterized curve in joint space. The trajectory planner receives these geometric paths as input and determines a time history of position, velocity, acceleration, and joint torques which are then fed to the *trajectory tracker*.

With the division outlined above, we have formulated in [8,9] the minimum time trajectory planning (MTTP) problem to determine controls which will drive a given manipulator along a specified curve in joint space in minimum time, given constraints on initial and final positions and velocities as well as on control signal magnitudes. Since a geometric path can be described as a parameterized curve, and the geometric path is assumed to be given, trajectory planning is relatively simple. By introducing a single parameter which describes the manipulator's position, the dimensionality of the problem has been reduced considerably. The current state (joint positions and velocities) of the manipulator can be described in terms of the parameter used to describe the geometric path and its time derivative. The MTTP problem is therefore essentially a two dimensional minimum time control problem with some state and input constraints.

More formally, assume that the geometric path is given in the form of a parameterized curve, say

$$q^i = f^i(\lambda), \quad 0 \leq \lambda \leq \lambda_{\max} \quad (1.1)$$

where q^i is the position of the i -th joint, and the initial and final points on the trajectory correspond to the points $\lambda = 0$ and $\lambda = \lambda_{\max}$, respectively. The functions f^i are continuous and differentiable, and their derivatives must be continuous

and piecewise differentiable. Also assume that the bounds on the actuator torques can be expressed in terms of the state of the system, i.e., the manipulator's speed and position, so that

$$u_i^{\min}(q, \dot{q}) \leq u_i \leq u_i^{\max}(q, \dot{q}) \quad (1.2)$$

where u_i is an n -dimensional vector of actuator torques/forces; u_i^{\max} and u_i^{\min} are n -dimensional vectors that represent the maximum and minimum torque bounds, respectively; and n is the number of joints that the manipulator has. (The vector inequality (1.2) denotes component-wise inequalities.) Given the functions f^i in Eq. (1.1), the inequality (1.2), the desired initial and final positions and velocities, and the manipulator dynamic equations to be given in Eq. (3.1), the MTTP problem is to find $q(\lambda)$ and $\dot{q}(\lambda)$, and hence the controls $u_i(\lambda)$ which minimize the traversal time T . See [8-10] for more detailed descriptions of our solution to the MTTP problem. Bobrow *et al* obtained similar solutions independently of ours [1].

In terms of the trajectory planning problem, the geometric path planning problem is the problem of picking the parametric functions f^i . In contrast to the trajectory planning problem, in which the desired solutions can be expressed in terms of the position parameter λ and its first and second time derivatives, the geometric path planning problem requires that a set of functions be chosen from an infinite dimensional space, thereby leading to a more difficult problem to solve.

In this paper, we will develop a method for determining an approximate minimum time geometric path for the trajectory planners described in [8,10]. This is a significant departure from most of the conventional planning methods in which geometric path planning [4,5] is performed without considering the robot's dynamic behavior. Specifically, we intend in this paper to consider the effects of actuator constraints and robot dynamics in both geometric path and trajectory planning.

This paper is organized as follows. In Section 2, we state formally the minimum time geometric path planning (MTGPP) problem to be solved in conjunction with trajectory planning. Section 3 discusses some interesting dynamic properties of manipulators that are useful for deriving solutions to the MTGPP problem. In Section 4, we present (i) an exact solution to the MTGPP problem under certain restricted conditions, (ii) a method for finding lower bounds on the traversal time from one point to another, and (iii) the paths which result from (a) minimizing the traversal time bounds and (b) maximizing the velocity bounds derived in [8,9]. Section 5 shows how our solutions are applied to the first three joints of a cylindrical manipulator, called the PACS arm, manufactured by the Bendix Corporation. The paper concludes with Section 6.

2. PROBLEM STATEMENT

The minimum time trajectory planning algorithms described in [8,10] give the time history of manipulator's position, velocity, and joint torques required for the minimum time traversal of a given geometric path. However, these algorithms give no firm indication of how to pick a geometric path. The chosen geometric path ideally should be that which avoids all obstacles and can be traversed with the minimum time. In conjunction with trajectory planning, the minimum time geometric path planning (MTGPP) problem can be stated as follows.

Problem MTGPP:

Given the solution to the minimum time trajectory planning problem, choose the geometric path, or the functions f^i in Eq. (1.1), so as to minimize the traversal time.

We will take approaches to this problem which are totally different from the conventional control techniques such as use of the Pontryagin's maximum principle. First, the minimum time path will be determined for a restricted class of robotic manipulators using some geometric techniques. Second, a method will be proposed for generating approximate minimum time geometric paths for more general manipulators. Note that these solutions are derived for collision-free space motions. Extension of the solutions to the case of obstacle avoidance is also indicated in the Conclusion. We begin in the next section with a few dynamic properties of manipulators that are needed.

3. DYNAMIC PROPERTIES OF MANIPULATORS

In this section we will introduce some properties of manipulators which will prove to be useful later on. Most of these properties relate to the "inertia space" of the manipulator, i.e., that Riemannian space which has the manipulator's inertia matrix as its metric tensor. The dynamic equations of a manipulator can be derived from Lagrange's equations, and take the form

$$u_i = J_{ij} \dot{v}^j + [jk, i] v^j v^k + R_{ij} v^j + g_i \quad (3.1)$$

where u_i is the generalized force/torque applied to the i -th joint, v^i is the generalized velocity of the i -th joint, J_{ij} is the inertia matrix, R_{ij} is the viscous friction matrix, and g_i is the gravitational force on the i -th joint. The summation convention has been used here, and all sums range from 1 to n for an n -jointed manipulator. It should also be noted that J_{ij} , R_{ij} , and g_i may in general be functions of the generalized coordinates q^i . The symbol $[jk, i]$ is a Christoffel symbol of the first kind, defined as

$$[jk, i] \equiv \frac{1}{2} \left(\frac{\partial J_{ij}}{\partial q^k} + \frac{\partial J_{ik}}{\partial q^j} - \frac{\partial J_{jk}}{\partial q^i} \right)$$

Eq. (3.1) can be written as

$$u_i = J_{ij} \frac{\delta v^j}{\delta t} + R_{ij} v^j + g_i \quad (3.2)$$

where $J_{ij} \frac{\delta v^j}{\delta t}$ is the absolute derivative of velocity with respect to time. (See [11] for more details.)

For our purposes, we will define arc length ds by the quadratic form $ds^2 \equiv J_{ij} dq^i dq^j$. Since the kinetic energy of the manipulator is given by $K = \frac{1}{2} J_{ij} \frac{dq^i}{dt} \frac{dq^j}{dt}$, it can be seen that the infinitesimal arc ds in this space is related to the kinetic energy of the manipulator by the formula

$$\left(\frac{ds}{dt} \right)^2 = 2K.$$

The dynamic equations may now be expressed in terms of the arc length s and the time derivatives of s . We have, since the absolute derivative obeys the chain rule,

$$u_i = J_{ij} \frac{\delta v^j}{\delta s} \frac{ds}{dt} + R_{ij} v^j + g_i \quad (3.3)$$

Using the relationship $v^j = \frac{dq^j}{ds} \frac{ds}{dt}$, then

$$u_i = J_{ij} \frac{\delta}{\delta s} \left(p^j \frac{ds}{dt} \right) \frac{ds}{dt} + R_{ij} p^j \frac{ds}{dt} + g_i \quad (3.4)$$

where $p^j \equiv \frac{dq^j}{ds}$ is the unit tangent to the manipulator's path. But

$$\frac{\delta}{\delta s} \left(p^j \frac{ds}{dt} \right) = \frac{\delta p^j}{\delta s} \frac{ds}{dt} + p^j \frac{\delta}{\delta s} \left(\frac{ds}{dt} \right) \quad (3.5)$$

Applying the product rule and chain rule to the absolute derivative in (3.5) and using the fact that the absolute

derivative of a scalar is just its ordinary derivative gives

$$u_i = J_{ij} \frac{\partial p^j}{\partial s} \left(\frac{ds}{dt} \right)^2 + J_{ij} p^j \frac{d^2 s}{dt^2} + R_{ij} p^j \frac{ds}{dt} + g_i. \quad (3.6)$$

The work W done on the manipulator is

$$W = \int u_i dq^i = \int u_i \frac{dq^i}{ds} ds = \int u_i p^i ds. \quad (3.7)$$

Plugging in the expression for u_i from Eq. (3.6),

$$W = \int \left[J_{ij} p^i \frac{\partial p^j}{\partial s} \frac{ds}{dt} + J_{ij} p^i p^j \frac{d}{ds} \left(\frac{ds}{dt} \right) \right] \frac{ds}{dt} ds + \int R_{ij} p^i p^j \frac{ds}{dt} ds + \int g_i p^i ds. \quad (3.8)$$

Using the facts that the curvature vector $\frac{\partial p^j}{\partial s}$ is orthogonal to the unit tangent p^j and that p^i is a unit vector, i.e., that $J_{ij} p^i p^j = 1$, Eq. (3.8) transforms to

$$W = \int \left(\frac{ds}{dt} \right) \frac{d}{ds} \left(\frac{ds}{dt} \right) ds + \int R_{ij} p^i p^j \frac{ds}{dt} ds + \int g_i p^i ds = \frac{1}{2} \left(\frac{ds}{dt} \right)^2 + \int R_{ij} p^i p^j \frac{ds}{dt} ds + \int g_i p^i ds. \quad (3.9)$$

The power consumed by the manipulator is just

$$P_i = \frac{dW}{dt} = \frac{ds}{dt} \frac{d^2 s}{dt^2} + R_{ij} p^i p^j \left(\frac{ds}{dt} \right)^2 + g_i p^i \frac{ds}{dt}. \quad (3.10)$$

4. MINIMUM TIME GEOMETRIC PATH PLANNING

As was previously pointed out, use of the maximum principle for solving the MTGPP problem is practically impossible. Alternative approaches must be sought. In this section we will develop three methods for generating geometric paths. For the first two we use energy methods to derive a lower bound on path traversal times, and for the third method we use the velocity limits derived in [8,9].

First it will be shown that geodesics in inertia space, i.e. solutions of the differential equations $\frac{\delta}{\delta s} \left(\frac{dq^i}{ds} \right)$, are

the optimal solutions to the MTGPP problem under some restricted conditions. Though the conditions required in the special case are not met by realistic manipulators, the proof does provide a simple illustration of the method used here for obtaining lower bounds on traversal time; the curves which minimize the lower bound for the more general case can then be found using essentially the same technique used in the special case, giving an absolute lower bound on the time required to move from one point to another. Then the use of the derived traversal time bounds and the velocity limits derived in [8,9] are used to find approximations to minimum time paths.

4.1. A Special Case

It will now be shown that if a manipulator has no friction terms and no gravitational terms and the limitations on the joint torques consist only of limits on the total power supplied to (or taken from) the manipulator, then the minimum time geometric paths are geodesics in inertia space. Formally, we have the following theorem:

Theorem 1: If a manipulator is frictionless and has zero gravitational terms, i.e. $R_{ij} = 0$ and $g_i = 0$ in the dynamic equations (3.1), and the only restrictions on the torques applied to the manipulator arise from constant, symmetric limits on the total power supplied to (or taken from) the manipulator, then the minimum-time geometric path

between any two configurations of the manipulator is a **geodesic** in inertia space provided that the initial and final velocities are zero.

Proof: The total power sunk or sourced by the manipulator is limited by symmetrical constant bounds, i.e., $-P_{\max} \leq P \leq P_{\max}$. Then by Eq. (3.10), applying the constant maximum power gives

$$P = P_{\max} = \frac{ds}{dt} \frac{d^2 s}{dt^2} = \mu \frac{d\mu}{dt} \quad (4.1)$$

where $\mu \equiv \frac{ds}{dt}$. Solving the differential Eq. (4.1) gives

$$\frac{1}{2} \mu^2 = t P_{\max}, \quad \text{or} \quad s = \frac{2}{3} \sqrt{2P_{\max}} t^{\frac{3}{2}} \quad (4.2)$$

since the manipulator starts at rest.

Obviously, minimizing the traversal time for a given path requires that we maximize the "velocity" $\frac{ds}{dt}$. This in turn requires that the power P be maximized. Therefore, the maximum distance s which can be traveled in time t is given by Eq. (4.2).

Looking now at the end of the curve, we wish to have zero velocity at the end of the motion. Again, since we wish to minimize the traversal time, we want to stop as quickly as possible, which requires that we *drain* energy from the system as fast as possible. Applying the minimum power, $\mu \frac{d\mu}{dt} = -P_{\max}$. Solving this equation gives

$$\frac{1}{2} \mu^2 = P_{\max}(T-t), \quad \text{or} \quad s = S - \frac{2}{3} \sqrt{2P_{\max}} (T-t)^{\frac{3}{2}} \quad (4.3)$$

where S is the total "length" of the curve which is to be traversed and T is the (unknown) time when the destination point is reached.

At some point in the middle of the curve there must be a switch from acceleration to deceleration. Let the time, distance, and velocity at this point be denoted by t_s , s_s and μ_s , respectively. Eqs. (4.2) and (4.3) must give identical results at the switching point, so we have

$$\mu_s^2 = 2P_{\max} t_s = 2P_{\max}(T-t_s) \quad (4.4a)$$

and

$$s_s = S - \frac{2}{3} \sqrt{2P_{\max}} (T-t_s)^{\frac{3}{2}} = \frac{2}{3} \sqrt{2P_{\max}} t_s^{\frac{3}{2}} \quad (4.4b)$$

Eliminating t_s from these equations gives

$$T = \left(\frac{9}{4P_{\max}} \right)^{\frac{1}{3}} S^{\frac{2}{3}} \quad (4.5)$$

The total time T increases monotonically with S , so minimum distance in inertia space is, in this case, equivalent to minimum time. Therefore the geodesic, being the curve of shortest "distance" between any two points, is the optimal geometric path. **Q.E.D.**

The conditions under which this proof of optimality applies are not realistic, particularly the condition that gravitational terms be absent. The proof of optimality depends on the absence of gravitational terms because the presence of such terms makes the power supplied to the manipulator a function of position rather than a function only of the kinetic energy of the manipulator. The requirement that the joint torques/forces be only constrained by a total power limit for the entire manipulator is also unrealistic. However, it is possible in practice to obtain bounds on the total available power for the more general case; in the next subsection, such bounds will be used to find bounds on traversal times.

4.2. Traversal Time Bounds

In this subsection, we show how energy methods similar to those used in the previous subsection may be used to obtain lower bounds on the time required to move from one point in the robot's workspace to another. We start with Eq. (3.10), the formula for P_i , the power supplied to the manipulator. If we write $P_k = \frac{ds}{dt} \frac{d^2s}{dt^2}$, $P_f = R_{ij} p^i p^j \left(\frac{ds}{dt} \right)^2$, and $P_g = g_i p^i \frac{ds}{dt}$, then we have

$$P_k = P_i - P_f - P_g. \quad (4.6)$$

We will find bounds on P_k by finding bounds on P_i , P_f , and P_g . But before computing these bounds, we need the following result:

Lemma 1: The 2-norm of the vector p is bounded by:

$$\frac{1}{\sqrt{\lambda_{\max}(J)}} = \frac{1}{f_M(J)} \leq \|p\|_2 \leq \frac{1}{f_m(J)} = \frac{1}{\sqrt{\lambda_{\min}(J)}} \quad (4.7)$$

where

$$f_m(J) = \min_{p \neq 0} \sqrt{\frac{p^T J p}{p^T p}}, \quad f_M(J) = \max_{p \neq 0} \sqrt{\frac{p^T J p}{p^T p}}$$

(The quadratic form $J_{ij} p^i p^j$ has been written in vector form as $p^T J p$.) $\lambda_{\min}(J)$ is the smallest eigenvalue of J for all positions q , and $\lambda_{\max}(J)$ is defined similarly.

Proof: Since p^i is a unit vector in inertia space, we have $J_{ij} p^i p^j = p^T J p = 1$. Then we have

$$1 = p^T J p = \frac{p^T J p}{p^T p} p^T p \geq \min_{p \neq 0} \left[\frac{p^T J p}{p^T p} \right] \|p\|_2^2$$

Likewise, we have

$$1 = p^T J p = \frac{p^T J p}{p^T p} p^T p \leq \max_{p \neq 0} \left[\frac{p^T J p}{p^T p} \right] \|p\|_2^2$$

Since J is positive definite and symmetric, its eigenvectors span R^n . Expanding p in terms of the eigenvectors of J shows that $f_m^2(J) = \lambda_{\min}(J)$ and $f_M^2(J) = \lambda_{\max}(J)$, which, combined with the above inequalities, proves the lemma.

Q.E.D.

We now compute bounds on the total applied power P_i . It will be assumed here that bounds on P_i arise from constant bounds on the joint torques and from constant bounds on the total applied power.¹ Then, we have

Lemma 2: If $\frac{ds}{dt} > 0$, then

$$\max \left\{ P_{\min}, -\zeta \frac{ds}{dt} \right\} \leq P_i \leq \min \left\{ P_{\max}, \zeta \frac{ds}{dt} \right\}$$

where P_{\min} and P_{\max} are the minimum and maximum powers that can be supplied to the robot, $\zeta = \frac{\|u_i^{\max}\|_2}{\sqrt{\lambda_{\min}(J)}}$, and $\|u_i^{\max}\|_2$ is the maximum 2-norm of the torque vector.

Proof: By definition, we have $P_i = u_i p^i \frac{ds}{dt}$. The component of the torque in the direction of motion, $u_i p^i$, can be bounded by

$$|u_i p^i| \leq \|u_i^{\max}\|_2 \|p^i\|_2 \leq \frac{\|u_i^{\max}\|_2}{\sqrt{\lambda_{\min}(J)}}. \quad (4.8)$$

We therefore have

¹Bounds of this form can easily be found from motor saturation torques and from limits on power supply currents and voltages.

$$P_i \geq \max \left\{ P_{\min}, \frac{-\|u_i^{\max}\|_2}{\sqrt{\lambda_{\min}(J)}} \frac{ds}{dt} \right\} = \max \left\{ P_{\min}, -\zeta \frac{ds}{dt} \right\}$$

and

$$P_i \leq \min \left\{ P_{\max}, \frac{\|u_i^{\max}\|_2}{\sqrt{\lambda_{\min}(J)}} \frac{ds}{dt} \right\} = \min \left\{ P_{\max}, \zeta \frac{ds}{dt} \right\}$$

Q.E.D.

Lemma 3: P_f is bounded by $\phi \mu^2 \leq P_f \leq \phi' \mu^2$

where $\phi = \frac{\lambda_{\min}(R)}{\lambda_{\max}(J)}$ and $\phi' = \frac{\lambda_{\max}(R)}{\lambda_{\min}(J)}$.

Proof: By an argument similar to that used to derive bounds on $\|p\|_2$, we have $\lambda_{\min}(R) \|p\|_2^2 \leq p^T R p \leq \lambda_{\max}(R) \|p\|_2^2$ so that, by Lemma 1,

$$\frac{\lambda_{\min}(R)}{\lambda_{\max}(J)} \leq p^T R p \leq \frac{\lambda_{\max}(R)}{\lambda_{\min}(J)} \quad (4.9)$$

Multiplying by μ^2 gives the desired result.

Q.E.D.

Lemma 4: The gravitational energy contribution P_g is bounded by $-\psi \frac{ds}{dt} \leq P_g \leq \psi \frac{ds}{dt}$ where $\psi = \frac{\|g_i\|_2}{\sqrt{\lambda_{\min}(J)}} \frac{ds}{dt}$.

Proof: We have

$$|g_i p^i| \leq \|g_i\|_2 \|p^i\|_2 \leq \frac{\|g_i\|_2}{\sqrt{\lambda_{\min}(J)}} \quad (4.10)$$

by Lemma 1. Multiplying by $\frac{ds}{dt}$ proves the lemma. **Q.E.D.**

Using bounds derived in Lemmas 2 through 4, we are now in a position to obtain bounds on P_k .

Lemma 5: If we define $\mu \equiv \frac{ds}{dt} > 0$,²

$$\begin{aligned} \max \left\{ P_{\min}, -\zeta \mu \right\} - \phi \mu^2 - \psi \mu \\ \leq P_k \leq \min \left\{ P_{\max}, \zeta \mu \right\} - \phi \mu^2 + \psi \mu \end{aligned}$$

Proving this Lemma is just a matter of plugging the bounds obtained in Lemmas 2 through 4 into Eq. (4.8b).

We can now determine maximum velocities, as was done in the previous subsection. We have the following theorem:

Theorem 2: If the initial and final velocities are zero then

$$\mu \leq \min \left\{ \mu_m, \frac{\psi + \zeta (1 - e^{-\mu T})}{\phi}, \frac{\psi + \zeta (e^{\mu(T-1)} - 1)}{\phi} \right\}$$

where T is the traversal time of the path and $\mu_m = \frac{\psi + \sqrt{\psi^2 + 4\phi P_{\max}}}{2\phi}$.

Proof: Consider two cases. In the first case, let P_k be limited by the joint torque bounds. Then we have $-\zeta \mu \leq P_i \leq \zeta \mu$ so that

$$-\phi \mu^2 - (\psi + \zeta) \mu \leq \mu \frac{d\mu}{dt} \leq -\phi \mu^2 + (\psi + \zeta) \mu \quad (4.11)$$

But then, since we are considering positive values of μ ,

$$-\phi \mu - (\psi + \zeta) \leq \frac{d\mu}{dt} \leq -\phi \mu + (\psi + \zeta). \quad (4.12)$$

We must have zero velocity at the beginning and end of the path. If the (as yet unknown) traversal time is T , then

²We proved $\mu > 0$ in [8].

$$\mu \leq \frac{\psi + \zeta}{\varphi} \left(1 - e^{-\mu t} \right) \quad (4.13a)$$

and

$$\mu \leq \frac{\psi + \zeta}{\varphi} \left(e^{\mu(T-t)} - 1 \right) \quad (4.13b)$$

In the second case, limits are imposed by the total power limits, i.e. $P_{\min} \leq P_t \leq P_{\max}$. Then we have

$$P_{\min} - \varphi \mu^2 - \psi \mu \leq \mu \frac{d\mu}{dt} \leq P_{\max} - \varphi \mu^2 + \psi \mu \quad (4.14)$$

Again, we are only considering positive values of μ ; since in general $P_{\min} < 0$, the lower bound in this inequality will always be less than zero. Therefore the roots of the lower bound occur for negative values of μ and we cannot place an upper bound on μ . On the other hand, the upper bound has a positive root. Since we are starting at $\mu = 0$, that value of μ for which $\frac{d\mu}{dt}$ goes to zero cannot be exceeded, and we have

$$\mu \leq \mu_m = \frac{\psi + \sqrt{\psi^2 + 4\varphi P_{\max}}}{2\varphi} \quad (4.15)$$

Since inequalities (4.13a), (4.13b), and (4.15) must all be met, the theorem follows. **Q.E.D.**

To find lower bounds on traversal times, consider a manipulator, call it the *super-manipulator*, for which the constraints on joint torques are such that Eqs. (4.13a), (4.13b) and (4.15) apply. Then the super-manipulator has limits only on the 2-norm of the tangential component of the torque vector and on the total kinetic energy. Since these constraints apply for the original manipulator, the old manipulator's realizable torques are a subset of the super-manipulator's, so that the super-manipulator can do anything that the original manipulator can do. Thus any path can be traversed by the super-manipulator at least as quickly as the actual manipulator could traverse it. Finding the minimum traversal time for the super-manipulator therefore gives a lower bound on the traversal time for the original manipulator.

Finding the lower bound on the traversal time T for the super-manipulator is simple. It is just a matter of finding a value of T such that the area under the velocity vs. time curve is equal to the geodesic distance S between the initial and final points. Formally, we have

Theorem 3: Let the times t_1 and t_2 be given by

$$t_1 = \frac{1}{\varphi} \log \left[\frac{\psi + \zeta}{\psi + \zeta - \varphi \mu_m} \right] \quad (4.16a)$$

and

$$t_2 = T - \frac{1}{\varphi} \log \left[\frac{\psi + \zeta + \varphi \mu_m}{\psi + \zeta} \right]. \quad (4.16b)$$

If t_1 and t_2 are both real and $t_1 \leq t_2$, then the minimum traversal time T for the super-manipulator can be found by solving the equation

$$S = \frac{\mu_m}{\varphi} - \frac{\mu_m}{\varphi} + \mu_m T - \frac{\mu_m}{\varphi} \log \left[\frac{\psi + \zeta + \varphi \mu_m}{\psi + \zeta} \right] - \frac{\mu_m}{\varphi} \log \left[\frac{\psi + \zeta}{\psi + \zeta - \varphi \mu_m} \right]. \quad (4.17)$$

If t_1 is not real or $t_1 > t_2$, then T can be found by solving the simultaneous equations

$$\frac{\psi + \zeta}{\varphi} (1 - e^{-\mu t_2}) = \frac{\psi + \zeta}{\varphi} (e^{\mu(T-t_2)} - 1) \quad (4.18a)$$

$$\frac{\psi + \zeta}{\varphi} \left[t_2 - \frac{1}{\varphi} (1 - e^{-\mu t_2}) \right] \quad (4.18b)$$

$$= S - \frac{\psi + \zeta}{\varphi} \left[\frac{1}{\varphi} (e^{\mu(T-t_2)} - 1) - (T - t_2) \right].$$

Proof: Finding the distance travelled, the area under the velocity vs. time curve, requires that we consider the two cases described above, which correspond to (i) the case in which the velocity limit μ_m is reached, and (ii) the case where it is not. Case (i) is relatively simple. First, we need to know the points where the curves described in (4.13a) and (4.13b) reach the limiting velocity μ_m . These times may be obtained from (4.13a) and (4.13b) by setting $\mu = \mu_m$ and solving for t . These times are just t_1 for (4.13a) and t_2 for (4.13b). Then the area under the velocity vs. time curve will be given by

$$\begin{aligned} S &= \int_0^{t_1} \frac{\psi + \zeta}{\varphi} (1 - e^{-\mu t}) dt \\ &+ \int_{t_1}^{t_2} \mu_m dt + \int_{t_2}^T \frac{\psi + \zeta}{\varphi} (e^{\mu(T-t)} - 1) dt \\ &= \frac{\mu_m}{\varphi} - \frac{\mu_m}{\varphi} + \mu_m T \\ &- \frac{\mu_m}{\varphi} \log \left[\frac{\psi + \zeta + \varphi \mu_m}{\psi + \zeta} \right] - \frac{\mu_m}{\varphi} \log \left[\frac{\psi + \zeta}{\psi + \zeta - \varphi \mu_m} \right]. \end{aligned} \quad (4.19)$$

Since S is linear in T , determining T is easy.

In case (ii), we have a single switching time t_s , and we may match positions and velocities as was done in the special case in the previous subsection. Matching velocities gives (4.18a). Matching positions gives

$$\begin{aligned} s_s &= \int_0^{t_s} \frac{\psi + \zeta}{\varphi} (1 - e^{-\mu t}) dt \\ &= S - \int_{t_s}^T \frac{\psi + \zeta}{\varphi} (e^{\mu(T-t)} - 1) dt \end{aligned} \quad (4.20)$$

which, when integrated, gives equation (4.18b) **Q.E.D.**

Unfortunately, Eqs. (4.20) cannot be solved for t_s in closed form. However, we can still use these equations to prove that T increases monotonically with S , and thus prove that the optimal path for the super-manipulator is a geodesic. This being known, the geodesic distance S between the initial and final points can be calculated, and Eq. (4.20) can be solved numerically.

Theorem 4: The minimum traversal time T for the super-manipulator increases monotonically with the geodesic length S of the traversed path.

Proof: To prove that T increases monotonically with S we will show that $\frac{dT}{dS} > 0$. If case (i) of Theorem 3 holds, then the result is obvious. Case (ii) is slightly more complicated. First, we differentiate (5.23a) and (4.20) with respect to the switching time t_s , giving

$$e^{-\mu t_s} = e^{\mu(T-t_s)} \left(\frac{dT}{dt_s} - 1 \right) \quad (4.21a)$$

$$\frac{\psi + \zeta}{\varphi} (1 - e^{-\mu t_s}) \quad (4.21b)$$

$$= \frac{dS}{dt_s} - \frac{\psi + \zeta}{\varphi} \left(\frac{dT}{dt_s} - 1 \right) \left(e^{\mu(T-t_s)} - 1 \right).$$

Solving (4.21 a) for $\frac{dT}{dt_s}$, plugging into (4.21 b), solving

(4.21 b) for $\frac{dS}{dt_s}$, and dividing $\frac{dS}{dt_s}$ by $\frac{dT}{dt_s}$ gives

$$\frac{dS}{dT} = \frac{\psi + \xi}{\varphi\varphi' \left[1 + e^{-\varphi\varphi'} e^{-\varphi(T-t_2)} \right] + \varphi e^{-\varphi\varphi'} \left[1 - e^{-\varphi(T-t_2)} \right]} \left[\varphi' \left[1 - e^{-\varphi\varphi'} \right] \right] \quad (4.22)$$

which is greater than zero. Q.E.D.

If the actual lower bound is required, then Eq. (5.23a) may be solved for T . To do this, we may make use of the equations for t_1 and t_2 . The maximum velocity μ_m can be varied in these equations until $t_1 = t_2 = t_s$; then this value of t_s can be used in (4.21 a), which can be solved for T .

4.3. Approximate Minimum Time Paths

In this subsection we consider two methods for generating geometric paths which are approximately minimum time. The first method uses the traversal time bounds derived in the previous section and the second method uses the velocity bounds derived in [8,9].

First, consider the lower bounds on traversal time. If these bounds are good estimates of the actual traversal times, then minimizing the lower bound should approximately minimize the traversal time. Since the lower bound increases monotonically with the geodesic length S of the traversed curve, geodesics (minimum-length curves) must minimize the lower bound. The "near optimal" paths may then be determined by solving the differential equations for a geodesic,

namely $\frac{\delta}{\delta s} \left[\frac{d\mathbf{q}^i}{ds} \right] = 0$. This method of generating near-

minimum time paths can be applied to most practical robots; however, it places no penalties on forces which are orthogonal to the traversed path, so that path curvature is not penalized. If any further constraints are applied which force the introduction of curvature terms, then ignoring the magnitude of the curvature terms could make the lower bound a poor estimate of the actual traversal time, causing a poor choice of path. The minimization of lower bounds leads to the selection of shortest-distance paths in inertia space, which could have corners at which the manipulator must come to a complete stop. Path segments of high curvature also slow the manipulator down. Thus it is necessary to strike a compromise between curves of shortest distance and curves of smallest curvature. (This naturally leads to the second method of generating near-minimum time geometric paths.)

In order to reach such a compromise, we choose as an objective function the product of the length of the curve and some measure of the total curvature. This, of course, requires some quantitative measure of both curvature and distance in an n -dimensional space where n is the number of manipulator joints. One obvious measure of total curvature is the reciprocal of the maximum velocity, as computed in [8,9]. If the path is expressed in terms of an arbitrary parameter λ , then the expression

$$\int_0^{\lambda_{\max}} \frac{d\lambda}{\mu_{\max}(\lambda)} \quad (4.23)$$

would appear to be a good choice, where $\mu = \lambda$ and $\mu_{\max}(\lambda)$ is the velocity limit at position λ . This expression is independent of the parameterization chosen, and increases both as the length of the curve increases and as the curvature increases.

In order to use (4.23), the value of the maximum velocity $\mu_{\max}(\lambda)$ is required. In [8,9] we have derived this bound in terms of the manipulator's torque bounds and its dynamic equations. The set of admissible accelerations μ is

given by a set of inequalities of the form

$$u_i^{\min} \leq M_i \mu + Q_i \mu^2 + R_i \mu + S_i \leq u_i^{\max} \quad (4.24)$$

where

$$M_i \equiv J_{ij} \frac{df^j}{d\lambda} \quad Q_i \equiv J_{ij} \frac{d^2 f^j}{d\lambda^2} + [j^k, i] \frac{df^j}{d\lambda} \frac{df^k}{d\lambda}$$

$$R_i \equiv R_{ij} \frac{df^j}{d\lambda} \quad S_i \equiv g_i$$

For a given position λ and velocity μ , these inequalities give a range of accelerations μ , and so may be thought of as assigning upper and lower acceleration bounds to each point (λ, μ) in the phase plane. Since these inequalities must hold for all joints of the manipulator, the acceleration must fall between the greatest of the lower acceleration bounds and the least of the upper bounds. When one of the upper acceleration bounds is smaller than one of the lower acceleration bounds for some phase point (λ, μ) , there are no accelerations which will keep the manipulator on the desired path. Thus the acceleration bounds generate restrictions on the velocities at the phase points which can be encountered during a traversal of the path. These relationships can be thought of as assigning velocity limits to a given position λ .

Now consider a frictionless manipulator, i.e. one for which the quantities R_i are zero. Also assume that at every point on the path the manipulator is capable of stopping and holding its position. Then we have

$$u_i^{\min} \leq S_i \leq u_i^{\max} \quad (4.25a)$$

at all points on the path. (This will hereafter be referred to as the "strong manipulator assumption".) If the parameter λ is defined to be the arc length s in inertia space, then Q_i is just the inertia matrix J_{ij} multiplied by the curvature vector $\frac{d^2 \mathbf{q}^j}{ds^2}$. But if the path chosen is a geodesic, the curvature vector is zero, and hence $Q_i \equiv 0$. Then the inequality (4.24) reduces to

$$u_i^{\min} \leq M_i \mu + S_i \leq u_i^{\max} \quad (4.25b)$$

which is independent of the velocity μ , and by the strong manipulator assumption is satisfied identically for $\mu = 0$. But if the bounds on μ are independent of μ , there can be no velocity limits; in other words, $\mu_{\max}(\lambda) = \infty$, so that the integrand of (4.23) is zero. Thus in this case the optimal solution coincides with that obtained from minimizing traversal times.

It may appear at first that the geodesic, since it maximizes velocity bounds, must be the true minimum time path. However, as shown in [8,9] the manipulator must meet acceleration as well as velocity constraints. It would then be expected that along the optimal geometric path the maximum acceleration would be maximized during an accelerating portion of the path and the minimum acceleration would be minimized during a decelerating portion. This does not happen along a geodesic, but a similar phenomenon occurs: the acceleration bounds "spread out". To see this, note that velocity limits occur because the acceleration bounds become very close. Since the velocity bounds have been eliminated by choosing a geodesic as the path, the acceleration bounds must never get close. Hence maximizing velocity bounds also gives a large range of accelerations to choose from. This would lead one to expect that geodesics are good, if not optimal, choices for geometric paths.

In summary, we have two criteria for selecting near-minimum time geometric paths for a manipulator, one based on the minimization of a lower bound on the manipulator's traversal time and the other based on the minimization of

the product of the path's length and its curvature. In either case, when the near-optimal path is determined, the path is found to be a geodesic in inertia space. This geodesic can be constructed by solving a set of differential equations and applying appropriate boundary conditions.

5. EXAMPLES

To demonstrate the utility of the solutions described above, the traversal times for various geometric path have been calculated, using the method of [8,9], for the Bendix PACS arm. This arm is cylindrical in configuration, and is driven by fixed-field D.C. motors. Only the dynamics of the first three joints are considered here (see Figure 1). We construct three paths, a straight line, a geodesic, and a joint-interpolated curve. (The joint-interpolated curve has the form $q^i = q_s^i + \lambda(q_f^i - q_s^i)$, where $0 \leq \lambda \leq 1$ and q_s^i and q_f^i are the points at which the curve starts and finishes.)

Both construction of geodesics and trajectory planning require that the dynamic equations (3.1) of the robot be known. In particular, the inertia matrix and Coriolis coefficients are needed in order to construct geodesics. For the first three joints of the manipulator the inertia matrix takes the form

$$J_{ij} = \begin{bmatrix} J_i - Kr + M_i r^2 & 0 & 0 \\ 0 & M_i & 0 \\ 0 & 0 & M_z \end{bmatrix} \quad (5.1)$$

where $q^1 = \psi$, $q^2 = r$, and $q^3 = z$. The constants M_i and M_z are the masses which the r and z axes must move. J_i is the moment of inertia around the ψ axis when r is zero. The K term is present because the center of mass of the structure for the r joint does not coincide with the ψ axis when r is zero. The values of J_i , K , M_i , and M_z , along with friction coefficients and actuator characteristics, may be found in [7]. The Christoffel symbols of the first kind (Coriolis coefficients) are found by differentiating J_{ij} . Those symbols which are non-zero are

$$[12,1] = [21,1] = M_i r - \frac{K}{2}, \quad [11,2] = \frac{K}{2} - M_i r \quad (5.2a)$$

The geodesics are solutions of the equations $0 = J_{ij} \frac{d^2 q^j}{ds^2} + [jk,i] \frac{dq^j}{ds} \frac{dq^k}{ds}$. Plugging Eqs. (5.1) through (5.2b) into this equation gives the equations of the geodesics as

$$0 = (J_i - Kr + M_i r^2) \frac{d^2 \psi}{ds^2} + (2M_i r - K) \frac{dr}{ds} \frac{d\psi}{ds} \quad (5.3a)$$

$$0 = M_i \frac{d^2 r}{ds^2} + \left(\frac{K}{2} - M_i r \right) \left(\frac{d\psi}{ds} \right)^2 \quad (5.3b)$$

$$0 = M_z \frac{d^2 z}{ds^2} \quad (5.3c)$$

In addition, we have the normality condition

$$(J_i - Kr + M_i r^2) \left(\frac{d\psi}{ds} \right)^2 + M_i \left(\frac{dr}{ds} \right)^2 + M_z \left(\frac{dz}{ds} \right)^2 = 1. \quad (5.4)$$

The geodesics are found by solving these equations numerically.

The gravitational terms for this manipulator are particularly simple; the gravitational forces on the r and ψ joints are zero, and the force on the z joint is $M_z g$.

Trajectory planning also requires knowledge of the robot's actuator characteristics. To determine actuator characteristics, consider a DC servo consisting of a voltage source, a resistance R^m , an inductance L , and an ideal motor, i.e., a device which generates a torque proportional to the current passing through it. The voltage source is the

power supply, the resistance is the sum of the voltage source resistance and the motor winding resistance, and the inductance is the inductance of the motor windings.

It will be assumed here that the inductance L can be neglected. This frequently is the case for D.C. motors, since the electrical time constant of such systems is generally much shorter than the mechanical time constant. Given that the torque τ is proportional to the current, i.e. $\tau = k^m I$, it can be shown from conservation of power that the voltage V_m across the ideal motor is just $k^m \omega$ where ω is angular velocity. Since, if the motor is not in saturation, $\tau = k^m I$ and $I = \frac{V_s - V_m}{R^m} = \frac{V_s - k^m \omega}{R^m}$ where V_s is the source voltage, we can solve for torque in terms of voltage and angular velocity, giving

$$\tau = \frac{k^m}{R^m} V_s - \frac{(k^m)^2}{R^m} \omega. \quad (5.5)$$

Assuming the power supply has constant voltage limits of V^{\min} and V^{\max} , this gives torque limits of

$$\frac{k^m}{R^m} V^{\min} - \frac{(k^m)^2}{R^m} \omega \leq \tau \leq \frac{k^m}{R^m} V^{\max} - \frac{(k^m)^2}{R^m} \omega. \quad (5.6a)$$

In addition, at some point the iron in the motor saturates, with the result that increasing the current through the motor has no effect on the torque. This yields two more (constant) torque limits, so we also require that

$$-\tau^{\text{sat}} \leq \tau \leq \tau^{\text{sat}} \quad (5.6b)$$

Taking the gear ratio k^g into account, this gives torque limits of

$$\omega^{\min} = \max \left\{ \frac{-\tau^{\text{sat}}}{k^g}, \frac{k^m}{R^m k^g} V^{\min} - \frac{(k^m)^2}{R^m (k^g)^2} \frac{dq^i}{d\lambda} \mu \right\} \quad (5.7a)$$

and

$$\omega^{\max} = \min \left\{ \frac{\tau^{\text{sat}}}{k^g}, \frac{k^m}{R^m k^g} V^{\max} - \frac{(k^m)^2}{R^m (k^g)^2} \frac{dq^i}{d\lambda} \mu \right\} \quad (5.7b)$$

A trajectory planner for this robot was written in the C programming language and run under the UNIX³ operating system on a VAX-11/780⁴. The trajectory planner was used to generate trajectories for a straight line, a geodesic, and a joint interpolated curve, each of which extended from the Cartesian point (0.7,0.7,0.1) to (0.4,-0.4,0.4), all coordinates being measured in meters. Phase plane plots (plots of the speed μ versus position λ), plots of position q^i vs. time, and plots of motor voltage vs. time are shown in Figures 2a through 4c. Figures 2a through 2c are for the straight line, Figures 3a through 3c are for the joint interpolated curve and Figures 4a through 4c are for the geodesic. The traversal times for these paths are 1.782, 1.796, and 1.588 seconds respectively, showing that the geodesic does indeed have the shortest traversal time.

6. CONCLUSIONS

Two methods (excluding the special case) have been proposed for finding geometric paths which allow a robotic manipulator to move from one point to another in minimum time or approximately minimum time; if obstacle avoidance is not a consideration, both methods yield the same result. While these methods do not directly address the problem of obstacle avoidance, they do demonstrate that the problem of choosing minimum time paths is not simple, and in particular they show that minimum time is not in general equivalent to minimum Cartesian distance.

³UNIX is a trademark of Bell Laboratories.

⁴VAX is a trademark of Digital Equipment Corporation.

Two approaches to the obstacle avoidance problem suggest themselves. If the geodesic which connects the desired initial and final positions of the manipulator happens to pass through an obstacle, then we may piece together geodesics to give a path which has shortest geodesic, rather than Cartesian, distance. This again has the disadvantage that the path will have corners at which the manipulator must stop, but these corners could presumably be rounded off, as in [6].

On the other hand, Eq. (4.23) provides a means of evaluating the "goodness" of any given path without actually calculating the path's traversal time. If several paths can be found which avoid collisions with obstacles, then each one can be evaluated and the best one chosen on the basis of formula (4.23). This presumes that some method can be developed for generating collision-free paths quickly. It also presumes that at least some of the paths generated by the algorithm are reasonably close to the optimal path. But since minimization of the product of curvature and distance gives paths with short traversal times, some guidelines for generating paths are now available.

REFERENCES

- [1] J. E. Bobrow, S. Dubowsky, and J. S. Gibson, On the Optimal Control of Robotic Manipulators with Actuator Constraints," *Proceedings of the 1983 Automatic Control Conference*, pp. 782-787, June 1983.
- [2] M. E. Kahn and B. Roth, The Near-Minimum-Time Control of Open-Loop Articulated Kinematic Chains," *ASME Journal of Dynamic Systems, Measurement, and Control*, pp. 164-172, September 1971.
- [3] B. K. Kim and K. G. Shin, Suboptimal Control of Industrial Manipulators with a Weighted Minimum Time-Fuel Criterion," *IEEE Trans. on Automatic Control*, vol. AC-30, no. 1, pp. 1-10, January 1985.
- [4] T. Lozano-Perez, Automatic Planning of Manipulator Transfer Movements," A. I. memo 606, MIT Artificial Intelligence Laboratory, December 1980.
- [5] T. Lozano-Perez, Spatial Planning: A Configuration Space Approach," A. I. memo 605, MIT Artificial Intelligence Laboratory, December 1980.
- [6] J. Y. S. Luh and C. S. Lin, Optimum Path Planning for Mechanical Manipulators," *ASME Journal of Dynamic Systems, Measurement, and Control*, vol. 102, pp. 142-151, June 1981.
- [7] K. G. Shin and N. D. McKay, Selection of Minimum Time Geometric Paths for Robotic Manipulators," CRIM technical memo #RSD-TR-17-84, Nov. 1984.
- [8] K. G. Shin and N. D. McKay, Minimum-Time Control of a Robotic Manipulator with Geometric Path Constraints," *Proceedings of the 22nd CDC*, pp. 1449-1457, Dec. 1983.
- [9] K. G. Shin and N. D. McKay, Minimum-Time Control of a Robotic Manipulator with Geometric Path Constraints," *IEEE Transactions on Automatic Control*, vol. AC-30, no. 6, June 1985.
- [10] K. G. Shin and N. D. McKay, Open-Loop Minimum-Time Control of Mechanical Manipulators and Its Application," *Proc. 1984 American Control Conference* pp. 1231-1236, June 6-8, 1984.
- [11] J. L. Synge and A. Schild, *Tensor Calculus*. New York: Dover Publications, 1978.

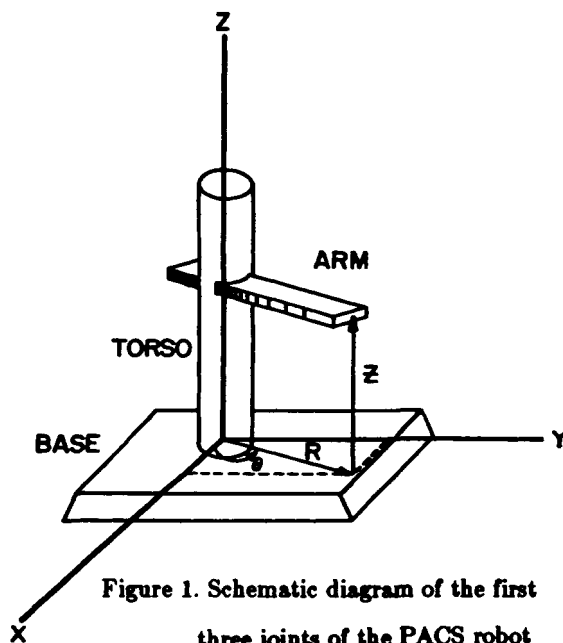


Figure 1. Schematic diagram of the first three joints of the PACS robot

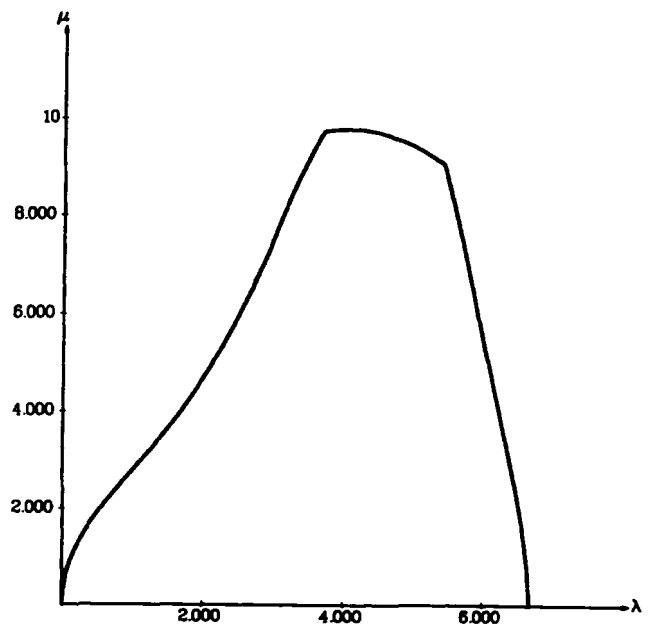


Figure 2a. Phase plane plot for straight line

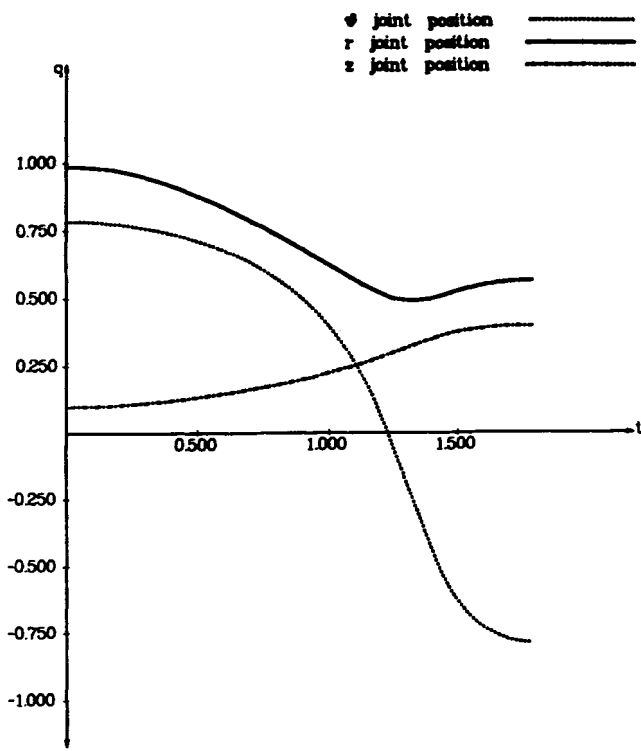


Figure 2b. Joint position vs. time for straight line

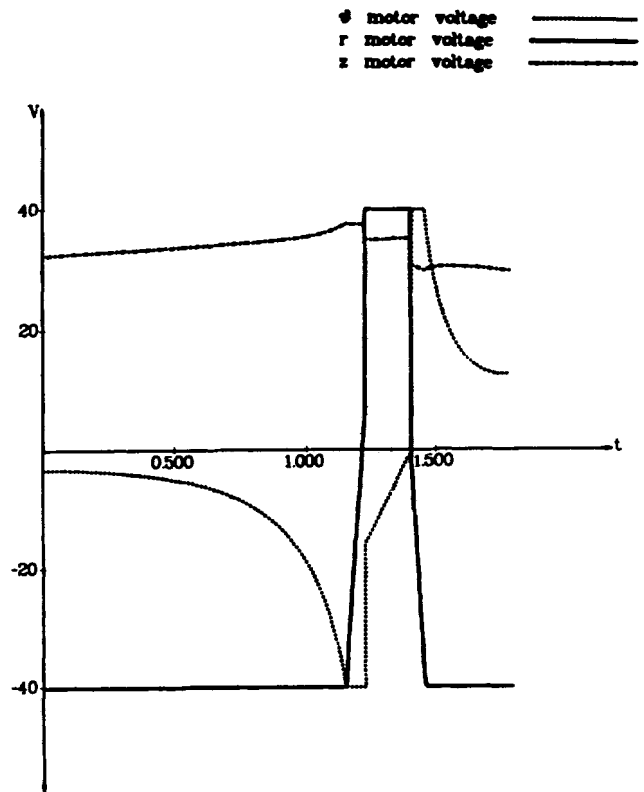


Figure 2c. Motor voltages vs. time for straight line

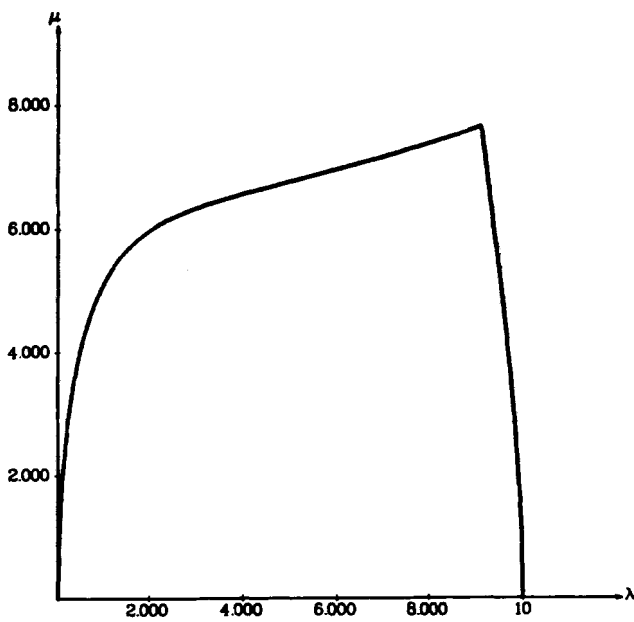


Figure 3a. Phase plane plot for joint-interpolated path

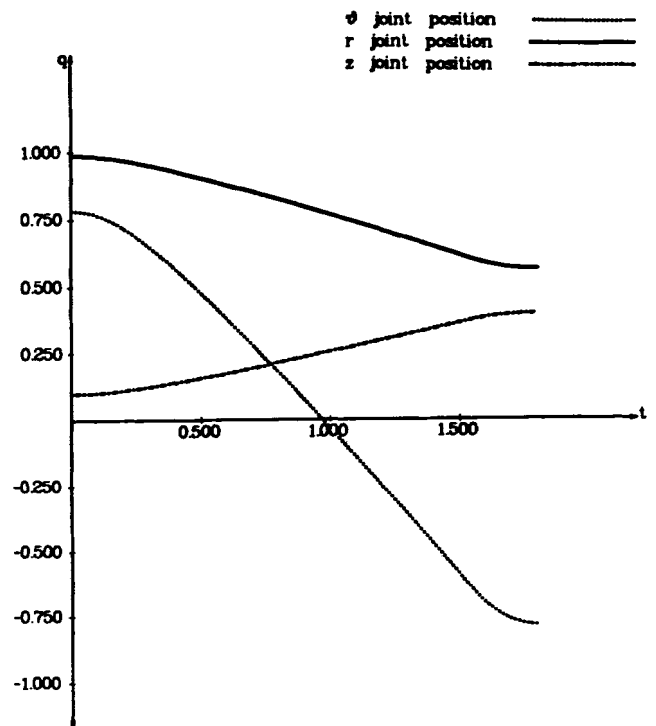


Figure 3b. Joint position vs. time for joint-interpolated path

